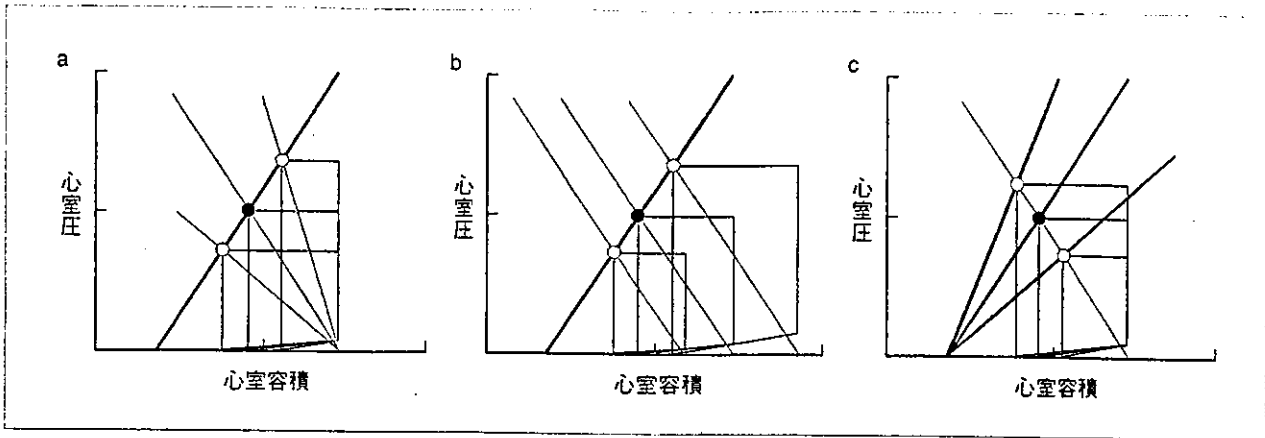

[図9] 心室動脈整合を用いた血行動態の解析
a 実効動脈エラスタンスの変化による血行動態の変化．実効動脈エラスタンスを増加させると収縮末期圧は増加し一回拍出量は減少する．実効動脈エラスタンスを低下させると収縮末期圧は低下し一回拍出量は増加する．
b 左室拡張末期容積の変化による血行動態の変化．左室拡張末期容積を増加させると収縮末期圧は増加し一回拍出量も増加する．左室拡張末期容積を減少させると収縮末期圧は低下し一回拍出量も減少する．
c 収縮性（E_{max}）の変化による血行動態の変化．収縮性を増加させると収縮末期圧は増加し一回拍出量も増加する．収縮性を低下させると収縮末期圧は低下し一回拍出量も減少する．
（文献 12）より引用改変）

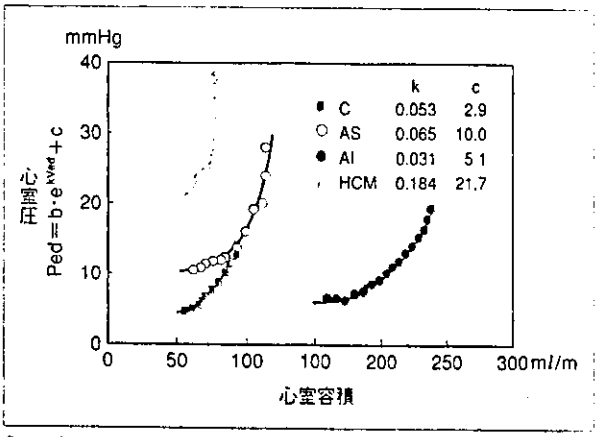

[図10] 拡張末期圧容積関係の例
C はコントロール，AS は大動脈弁狭窄症，AI は大動脈弁逆流症，HCM は肥大型心筋症を表す．拡張末期圧容積関係は AS，HCM の症例で上方に移動しており，一方，AI の症例では右方に移動している．心室の硬さを示す k は AS，HCM の症例で増加し，AI の症例で減少している．（文献 17）より引用）

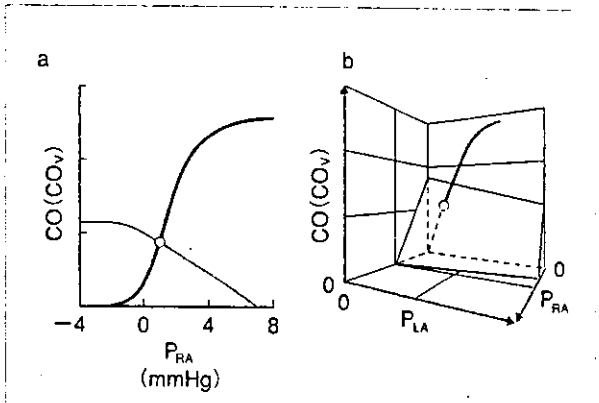

[図11] 循環平衡の概念
a Guyton らの循環平衡．体血管系がある右心圧（P_{RA}）のもとでどれだけの血流量を心臓および肺血管系に戻すことができるか（静脈還流量，CO_V）を表したものが静脈還流曲線である．右房圧が増加すると静脈還流量は減少する．一方，心臓および肺血管系がある右房圧によってどれだけの心拍出量（CO）を全身へ送り出すかを表したものが心拍出量曲線である．Frank-Starling 機構により右房圧が増加すると心拍出量は増加する．両曲線の交点（循環平衡点）から心拍出量と右房圧が決定される．
b 筆者らの提唱する循環平衡．体血管系と肺血管系がある左右の心房圧（P_{LA}，P_{RA}）に対してどれだけの血流量を心臓に戻すことができるか（静脈還流量，CO_V）を表したものが静脈還流平面である．一方，左右心室がある左右の心房圧に対してどれだけの心拍出量（CO）を全身へ送り出すかを表したものが統合心拍出量曲線である．平面と曲線の交点から心拍出量と左右の心房圧が決定される．
（文献 19）より引用）

での心不全では機械的効率は低下するが外的仕事がほぼ最大な条件で動作していた．心不全が重症化すると外的仕事も機械的効率も低下した．Kimらは拡張型心筋症の臨床例において予後と心室機能の関係を検討した[16]．機械的効率，左室駆出率，拡張末期圧が単変量解析で予後との相関が強く，多変量解析では機械的効率が予後との相関が最も強かった．機械的効率が11%を下回ると生命予後が悪くなると報告している．

7. 圧容積関係による拡張期心室特性の評価

拡張末期圧容積関係

拡張期心室特性として拡張早期の能動的心室弛緩特性と拡張末期の心室の受動的伸展特性が重要である．前者は主に等容性弛緩期における心室内圧下降の時定数により評価される．一方，後者は拡張末期圧容積関係 end-diastolic pressure-volume relationship (EDPVR) によって評価される．EDPVRは非線形であり，以下のような指数関数に近似されることが多い．

$$P_{ed} = b \cdot e^{kVed} + c$$

ここで，P_{ed} は拡張末期圧，V_{ed} は拡張末期容積，bは圧のゲイン，cは圧のオフセット，kは非線形性の程度を表し心室の硬さである材料特性を表す定数である．これを V_{ed} について解くと対数関数が得られる．

$$V_{ed} = \frac{1}{k}[\ln(P_{ed} - c) - \ln(b)] \qquad (式2)$$

図10にさまざまな心疾患における左室のEDPVRの例を示す．

8. 心室圧容積関係に基づく血行動態の予測ー Guytonの理論を拡張した新しい循環平衡の枠組みー

循環平衡

心拍出量と左房圧は，Forresterの分類にも示されているように，心不全管理において重要である．治療によりこれらがどのように変化するかを定量的に予測できれば，心不全管理のうえできわめて有用である．心拍出量の制御メカニズムを解析するためGuytonらは，循環平衡の基本的枠組みを確立した[18]（図11a）．筆者らはこの枠組みを拡張し，心拍出量，右房圧に加え左房圧を変数とする新たな循環平衡の枠組みを考案し，麻酔下のイヌにてこの枠組みの妥当性を実証した．この枠組みでは，静脈還流量は肺血管系および体血管系の有効血液量の和によって変化し，心拍出量，右房圧，左房圧を三つの軸とする3次元図表上で一つの平面（静脈還流平面）として表される（図11b）．この静脈還流平面に，左右心室の心拍出量曲線を統合した曲線（統合心拍出量曲線）を交差させることで平衡点の心拍出量，左右の心房圧を求めることができる．

圧容積関係に基づく統合心拍出量曲線の同定と血行動態の予測

筆者らは圧容積関係に基づいて心拍出量曲線をモデル化しそのパラメータを推定する方法を考案した．心拍出量（CO）は一回拍出量（SV）と心拍数（HR）から計算でき，（式2）の対数関数を用いると，COは次のように左房圧（P_L）の対数関数となる．

$$CO = S_L \times [\ln(P_L - F_L) + H_L]$$

定数 S_L は曲線の傾きを規定しており，ほかの2係数は標準値を用いることで，一組の心拍出量，左房圧から S_L を求めることができる．この方法によって良好な精度で心拍出量を推定することができた[20]．また同定された統合心拍出量曲線と静脈還流平面を交差させることにより正確に心拍出量および左右の心房圧の変化を予測することができた．この結果はスワンガンツカテーテルにて計測される血行動態から静脈還流平面と心拍出量曲線，治療による血行動態の変化を定量的に予測できることを意味する．この枠組みは強力な循環不全の管理指針として今後展開するものと期待される．

おわりに

以上に述べたように心室の圧容積関係を用いる

ことにより，収縮性，心室動脈結合，拡張性の評価，さらには収縮効率，外的仕事，機械的効率の検討が可能となった．また循環平衡理論により血行動態の定量的予測が可能となった．今後これらのアプローチが，種々の病態の理解や適切な循環管理，新たな治療法の進歩に貢献することが期待される．

文献

1) Baan, J et al : Continuous measurement of left ventricular volume in animals and humans by conductance catheter. Circulation 1984 ; 70 : 812-823
2) Tulner SA et al : Perioperative assessment of left ventricular function by pressure-volume loops using the conductance catheter method. Anesth Analg 2003 ; 97 : 950-957
3) Uemura, K et al : Self-calibratable ventricular pressure-volume telemetry system for rats. (abstract) Circulation 2003 ; 108 : IV-37
4) Suga, H et al : Instantaneous pressure-volume relationships and their ratio in the excised, supported canine left ventricle. Circ Res 1974 ; 35 : 117-126
5) Suga, H et al : Load independence of the instantaneous pressure-volume ratio of the canine left ventricle and effects of epinephrine and heart rate on the ratio. Circ Res 1973 ; 32 : 314-322
6) Kass, DA et al : Determination of left ventricular end-systolic pressure-volume relationships by the conductance (volume) catheter technique. Circulation 1986 ; 73 : 586-595
7) Shishido, T et al : Single-beat estimation of end-systolic elastance using bilinearly approximated time-varying elastance curve. Circulation 2000 ; 102 : 1983-1989
8) Burkhoff, D et al : Contractility-dependent curvilinearity of end-systolic pressure-volume relations. Am J Physiol 1987 ; 252 : H1218-H1227
9) Suga, H : Ventricular energetics. Physiol Rev 1990 ; 70 : 247-277
10) Takaoka, H et al : Comparison of hemodynamic determinants for myocardial oxygen consumption under different contractile states in human ventricle. Circulation 1993 ; 87 : 59-69
11) Sunagawa, K et al : Left ventricular interaction with arterial load studied in isolated canine ventricle. Am J Physiol 1983 ; 245 : H773-H780
12) Sagawa, K et al : Cardiac Contraction and Pressure-Volume Relationship, Oxford University Press, New York, 1988, 232-298
13) Sunagawa, K et al : Optimal arterial resistance for the maximal stroke work studied in isolated canine left ventricle. Circ Res 1985 ; 56 : 586-595
14) Burkhoff, D et al : Ventricular efficiency predicted by an analytical model. Am J Physiol 1986 ; 250 : R1021-R1027
15) Asanoi, H et al : Ventriculoarterial coupling in normal and failing heart in humans. Circ Res 1989 ; 65 : 483-493
16) Kim, IS et al : Prognostic value of mechanical efficiency in ambulatory patients with idiopathic dilated cardiomyopathy in sinus rhythm. J Am Coll Cardiol 2002 ; 39 : 1264-1268
17) Mandinov, L et al : Diastolic heart failure. Cardiovasc Res 2000 ; 45 : 813-825
18) Guyton, AC : Determination of cardiac output by equating venous return curves with cardiac response curves. Physiol Rev 1955 ; 35 : 123-129
19) Uemura, K et al : A novel framework of circulatory equilibrium. Am J Physiol Heart Circ Physiol 2004 ; 286 : H2376-H2385
20) 上村和紀ほか：心不全において血行動態を予測しうる新たな循環平衡の枠組み．第18回生体・生理工学シンポジウム論文集，2003, 379-380

（上村和紀・杉町　勝）

Prediction of circulatory equilibrium in response to changes in stressed blood volume

Author: Kazunori Uemura[1], Toru Kawada[1], Atsunori Kamiya[1], Takeshi Aiba[1,2], Ichiro Hidaka[1,3], Kenji Sunagawa[4], and Masaru Sugimachi[1]

Affiliations: [1]Department of Cardiovascular Dynamics, National Cardiovascular Center Research Institute, Suita 565-8565, Japan
[2]Pharmaceuticals and Medical Devices Agency, Tokyo 100-0013, Japan
[3]Japan Association for the Advancement of Medical Equipment, Tokyo 113-0033, Japan
[4]Department of Cardiovascular Medicine, Kyushu University Graduate School of Medical Science, Fukuoka 812-8582, Japan

Running Head: Estimating cardiac output curve by single hemodynamics

Word count: 5050

Correspondence: Kazunori Uemura, MD
Department of Cardiovascular Dynamics
National Cardiovascular Center Research Institute
5-7-1 Fujishirodai, Suita 565-8565, Japan
TEL +81-6-6833-5012 (Ext. 2466), FAX +81-6-6835-5403
E-mail: kuemura@ri.ncvc.go.jp

ABSTRACT

Accurate prediction of cardiac output (CO), left atrial pressure (P_{LA}) and right atrial pressure (P_{RA}) is a prerequisite for the management of patients with compromised hemodynamics. In our previous study (*Am J Physiol* 286; H2376, 2004), we have demonstrated a circulatory equilibrium framework, which permits the prediction of CO, P_{LA}, and P_{RA} once the venous return surface and integrated CO curve are known. As we have also shown that the surface can be estimated from single-point CO, P_{LA}, and P_{RA} measurements, we hypothesized that a similar single-point estimation of the CO curve would enable us to predict hemodynamics. In 7 dogs, we measured the P_{LA}-CO and P_{RA}-CO relationships and derived a standardized CO curve using the logarithmic function $CO=S_L[\ln(P_{LA}-2.03)+0.80]$ for the left heart and $CO=S_R[\ln(P_{RA}-2.13)+1.90]$ for the right heart, where S_L and S_R represent the preload sensitivity of CO, i.e., pumping ability, of the respective hearts. To estimate the integrated CO curve in each animal, we calculated S_L and S_R from single-point CO, P_{LA} and P_{RA} measurements. Estimated and measured CO agreed reasonably well. In another 8 dogs, we altered stressed blood volume (-8 to +8 $ml \cdot kg^{-1}$ of reference volume) under normal and heart-failing conditions, and predicted the hemodynamics by intersecting the surface and the CO curve thus estimated. We could predict CO ($y=0.93x+6.5$, $r^2=0.96$, SEE=7.5 $ml \cdot min^{-1} \cdot kg^{-1}$), P_{LA} ($y=0.90x+0.5$, $r^2=0.93$, SEE=1.4 mmHg), and P_{RA} ($y=0.87x+0.4$, $r^2=0.91$, SEE=0.4 mmHg) reasonably well. In conclusion, single-point estimation of the integrated CO curve enables accurate prediction of hemodynamics in response to extensive changes in stressed blood volume.

Key words: logarithmic function, venous return surface, heart failure, stressed blood volume

INTRODUCTION

Accurate prediction of cardiac output (*CO*) and cardiac filling pressures following therapeutic interventions is indispensable for optimal management and improving prognosis of patients with compromised hemodynamics (4, 5, 13, 23). In the 1980's, Sunagawa's group (20, 27) extended Guyton's (9, 10) framework of circulatory equilibrium to analyze complicated hemodynamic conditions such as left-sided heart failure. The extended framework is composed of a venous return surface representing the venous return of the systemic and pulmonary circulations, and an integrated cardiac output curve representing the pumping ability of the left and the right heart (Fig. 1) (27). The intersection point of the venous return surface and the integrated cardiac curve gives the equilibrium *CO*, left atrial pressure (P_{LA}) and right atrial pressure (P_{RA}). Changes in stressed blood volume shift the venous return surface upward or downward, altering the equilibrium point accordingly.

Our previous study (29) experimentally validated that venous return is a linear function of both P_{LA} and P_{RA}, and that this relationship is expressed by a flat surface, i.e., the venous return surface (Fig. 1). In addition, due to the small intra- and inter-animal variability in the slope of the surface, only a single set of *CO*, P_{LA} and P_{RA} values is sufficient to estimate the venous return surface. Furthermore, it is possible to predict how the venous return surface shifts in response to a known amount of change in the stressed blood volume. These findings suggest that if the integrated cardiac output curve can be estimated from a single set of *CO*, P_{LA} and P_{RA} values, it is possible to predict hemodynamics in response to various therapeutic interventions, which induce changes in loading condition or changes in the pumping ability of the heart (29). The present study was therefore undertaken to develop a method to estimate the integrated cardiac output curve from a single set of *CO*, P_{LA} and P_{RA} values, and to examine whether intersection of the

integrated cardiac output curve and the venous return surface thus estimated predicts hemodynamics in response to extensive changes in the stressed blood volume. Using our model, we were able to estimate the cardiac output curve and predict the hemodynamics in anesthetized, open-chest dogs under conditions of left heart failure as well as normal cardiac function.

METHODS

Integrated cardiac output curve

In our previous study, we showed that CO is closely related to P_{LA} or P_{RA} by a three-parameter logarithmic function (29):

$$CO = S_L \times [\ln(P_{LA} - F_L) + H_L] \quad (1)$$

$$CO = S_R \times [\ln(P_{RA} - F_R) + H_R] \quad (2)$$

where S_L, F_L, H_L, and S_R, F_R, H_R are parameters.

To estimate the integrated cardiac output curve from a single set of CO, P_{LA} and P_{RA} values, we fixed the F and H parameters according to the following rationale. It is well known that cardiac output curve varies widely with changes in ventricular contractility, heart rate, vascular resistance and diastolic stiffness (8, 10, 20, 21, 24, 30). As shown in Appendix, these factors are mainly included in the S parameter rather than the F or H parameters. The S parameter thus comprehensively represents the pumping ability of the left heart or the right heart. Therefore, we hypothesized that variations in the cardiac output curve can be explained exclusively by the S parameter. Once standard values of F and H parameters are determined, we can estimate the integrated cardiac output curve by calculating the S parameter from a single set of CO, P_{LA} and

P_{RA} values.

Animal preparation

We used 15 adult mongrel dogs (both sexes, weight 20-30 kg). Care of the animals was in strict accordance with Guiding Principles for the Care and Use of Animals in the Field of Physiological Sciences, approved by the Physiological Society of Japan. Anesthesia was induced with sodium pentobarbital (25 mg/kg) and endotracheal intubation was performed. Isoflurane (1.5 %) was continuously inhaled to maintain an appropriate level of anesthesia during the experiment. Catheters (6F) were placed in the right femoral artery and vein for withdrawal of blood and for administration of drugs and fluids. To stabilize autonomic tone, we isolated the carotid sinuses bilaterally and maintained the intrasinus pressure constant at 120 mmHg (22). The cervical vagosympathetic trunks were cut. Systemic arterial pressure was measured by a catheter-tipped micromanometer (PC-751, Millar Instruments, Houston, TX) placed in the ascending aorta via the right carotid artery. After a median sternotomy, a small pericardial incision was made at the level of the aortic root. An ultrasonic flow-meter (20A594, Transonics, Ithaca, NY) was placed around the ascending aorta via the incision to measure *CO*. Fluid-filled catheters were placed in the left and right atria via the incision to measure P_{LA} and P_{RA}, respectively. They were connected to pressure transducers (DX-200, Nihon Kohden, Tokyo, Japan). The junction between the inferior vena cava and the right atrium was taken as the reference point for zero pressure (22).

Experimental protocol

Under normal control conditions, we first infused about 250 ml of 10% dextran solution via the right femoral vein. We withdrew blood from the femoral artery in steps of 2 ml·kg^{-1} up to a total volume of 16 to 22 ml·kg^{-1} (8 to 11 steps per animal). In each step, after waiting for 1 min, we recorded CO, P_{LA}, and P_{RA} for about 10 sec (Fig. 2). We assumed that this volume reduction alters only the stressed blood volume of the systemic and pulmonary circulation. Because we isolated the baroreceptors, baroreflex-related changes in unstressed blood volume were negligible. We defined the reference values of CO, P_{LA} and P_{RA} when half of the volume reduction was attained.

To create left ventricular failure, we embolized the left circumflex coronary artery with glass microspheres (90 μm in diameter) (28). We adjusted the amount of microspheres injected so as to increase P_{LA} by 20 mmHg. We then volume loaded the animals and repeated the above protocol.

The data recordings were done while respiration was temporarily suspended at end-expiration. All analog signals were digitized at 200 Hz with a 12-bit analog to digital converter (AD12-16UE, Contec, Osaka, Japan), using a dedicated laboratory computer system (MA 20V, NEC, Tokyo, Japan) and stored on a hard disk for subsequent analysis. All the recorded data were averaged over 5 seconds. All data presented, except for pressure data, were normalized to individual body weight.

Data analysis

Determination of standard values of F and H parameters We determined the standard values of F and H parameters in 7 randomly selected dogs (*Group 1*). We fitted the P_{LA}-CO and P_{RA}-CO

relationships obtained under normal conditions to the 3-parameter logarithmic functions (*Eq. 1 and 2*) using the least square method. We averaged the F and H values of the left and the right heart for the 7 animals. The averaged values were used as the standard F and H parameters in subsequent analyses.

Estimation of the integrated cardiac output curve Using the standard F and H parameters, we examined whether we could estimate the integrated cardiac output curve from a single set of CO, P_{LA} and P_{RA} values. For each animal in *Group 1*, we calculated the S parameter by substituting the reference values of CO, P_{LA} and P_{RA} into *Eq. 1* and *2*. This calculation was done under normal and heart failure conditions. After calculating the S parameter, the P_{LA} and P_{RA} measured in each step were substituted into *Eq. 1* to estimate CO of the left heart and into *Eq. 2* to estimate CO of the right heart, respectively. The estimated and measured CO were compared by linear regression analyses.

Prediction of circulatory equilibrium In the other 8 dogs (*Group 2*), we estimated both the integrated cardiac output curve and venous return surface. The cardiac output curve was estimated as described above, using the standard F and H parameters. Venous return surface was estimated according to our previous work (29) using the following formula.

$$CO_V = V/0.129 - 19.61P_{RA} - 3.49P_{LA} \qquad (3)$$

where V is the stressed blood volume, CO_V is the integrated venous return, and *0.129* (min), *19.61* ($ml \cdot min^{-1} \cdot kg^{-1} \cdot mmHg^{-1}$), *3.49* ($ml \cdot min^{-1} \cdot kg^{-1} \cdot mmHg^{-1}$) are standard parameters characterizing the venous return surface (29). The reference CO, P_{LA} and P_{RA} values were used to calculate V, which served as the reference stressed volume.

With altered V (from +8 to −8 ml·kg^{-1} of the reference value), we numerically determined the intersection of the venous return surface (*Eq. 3*) and the integrated cardiac output curve (*Eq. 1* and *2*) to predict CO, P_{LA} and P_{RA}. The predicted CO, P_{LA} and P_{RA} were compared with those measured. We considered the change in V (± 8 ml·kg^{-1}) as substantial, considering the physiological amount of the stressed blood volume (~25 ml·kg^{-1}) (17).

Statistics

Group data are expressed as means (SD). The level of statistical significance was defined as $p < 0.05$. To test the goodness of fit, the coefficient of determination (r^2) and the standard error of estimate (SEE) were calculated.

RESULTS

Determination of the standard parameters

Figure 3 shows the measured P_{LA}-CO (panel A) and P_{RA}-CO (panel B) relationship in a representative dog. Cardiac output increases in response to increases in either left or right atrial pressure by the Frank-Starling mechanisms. These relationships could be fitted to the 3-parameter logarithmic function (thin solid lines) (Fig. 3A, CO=66.7[ln(P_{LA}-2.08)+0.1], r^2 = 0.98, SEE = 5.9 ml·min^{-1}·kg^{-1}; Fig. 3B, CO=112.7[ln(P_{RA}-1.39)+0.19], r^2 = 0.98, SEE = 5.5 ml·min^{-1}·kg^{-1}).

Table 1 summarizes the results of the fit in 7 dogs. As shown in Tables 1-1 and 1-2, coefficients of determination were high for both the left (r^2=0.95-0.99) and the right heart (r^2=0.90-0.99). These results indicated that the logarithmic functions represented the cardiac

output curves of the left and the right heart with good accuracy. The averaged F and H values (F_L = 2.03 mmHg, H_L = 0.80, F_R = 2.13 mmHg and H_R = 1.90) for 7 animals were used as standard values in subsequent analyses.

Estimation of the integrated cardiac output curve

Figure 4 shows the estimated cardiac output curves under normal (solid lines) and heart failure conditions (dashed lines) of a single animal (Panel A; left heart, Panel B; right heart). Solid circles (normal) and solid squares (heart failure) indicate the reference hemodynamic values. From these reference values, we calculated individual values of the S parameter. Under normal conditions, the estimated cardiac output curve accurately coincided with the measured points (solid lines vs. open circles) in the left and in the right heart. A good agreement was also observed under left ventricular failure (dashed lines vs. open squares).

Figure 5 demonstrates the relationship between estimated and measured cardiac output of pooled data from 7 animals (*Group 1*). The estimated cardiac output agreed with the measured cardiac output in the left heart (Fig. 5A, y = 0.88 x + 13.3, n = 104, r^2 = 0.93, SEE = 8.7 ml·min^{-1}·kg^{-1}), and in the right heart (Fig. 5B, y = 0.96 x + 5.0, n = 104, r^2 = 0.88, SEE = 12.1 ml·min^{-1}·kg^{-1}).

Prediction of circulatory equilibrium

Figure 6 illustrates the accuracy of prediction of hemodynamics in response to changes in stressed blood volume (8 dogs, *Group 2*).

Figure 6A shows the relationship between predicted and measured cardiac output.

Cardiac output was predicted accurately (y=0.93x+6.5, n=128, r^2 = 0.96, SEE = 7.5 ml·min^{-1}·kg^{-1}) over a wide range of cardiac output from 30 to 200 ml·min^{-1}·kg^{-1}. A small intercept value with a nearly unity slope also indicates the accuracy of prediction.

Figure 6B shows the accuracy of the left atrial pressure prediction. Although variability increased in the high pressure range (> 20 mmHg), the prediction was reasonably accurate (y = 0.90 x + 0.5, n = 128, r^2 = 0.93, SEE = 1.4 mmHg).

Likewise, right atrial pressures were also predicted with reasonable accuracy (Figure 6C, y = 0.87 x + 0.4, n = 128, r^2 = 0.91, SEE = 0.4 mmHg).

DISCUSSION

The results of this study indicate that, once a single set of steady-state *CO*, P_{LA} and P_{RA} values is available, it is possible to predict the changes in hemodynamic variables resulting from a known amount of change in stressed blood volume. This prediction can be very helpful in the management of patients under unstable hemodynamic conditions (13, 23).

Estimation of the integrated cardiac output curve

We have shown that the integrated cardiac output curve can be estimated with reasonable accuracy under normal and heart failure conditions (Figs. 4 and 5). By fixing the *F* and *H* parameters and by ascribing the changes in the cardiac output curve exclusively to the *S* parameter, we were able to estimate the integrated cardiac output curve from a single set of hemodynamic measurements. As shown in Appendix, the *F* and *H* parameters are mainly related to end-diastolic pressure-volume relationship (*Eq. A4*). In advanced cardiac disorders seen

clinically, the end-diastolic pressure-volume relationship may vary drastically (6, 7). Hypertensive or idiopathic cardiomyopathy sometimes induces severe ventricular hypertrophy, thereby significantly altering the diastolic ventricular pressure-volume relationship (14). In such cases, it may be desirable not to use fixed values, but to estimate F and H parameters in individual patients. The cardiovascular properties shown in *Eq. A4* can be estimated non-invasively under a steady-state hemodynamic condition (3, 12). Integration of these properties into our method may allow independent estimation of the three parameters in individual patients.

The following validations indicate that our mathematical model of the cardiac output curve and its estimation are consistent with previous investigations. First, based on *Eq. A4* (see Appendix), we calculated the 3 parameters in the logarithmic function for the left heart using previously reported data (6, 11, 18, 25). The values of the cardiovascular properties were chosen to be appropriate for a 20 kg dog (Table 2). The calculated S_L (34 ml·min^{-1}·kg^{-1}), F_L (3.2 mmHg), and H_L (1.14) were compatible with those obtained in our experiment (Table1-1). Second, Pouleur et al. (19) examined the cardiac output curve of the left heart in dogs under various cardiac conditions (control, coronary occlusion, nitroprusside infusion under control and coronary occlusion). Their cardiac output curves could be approximated to our three-parameter logarithmic functions with reasonable accuracy (r^2 = 0.94-0.99). When we applied the standard values of F_L (2.03 mmHg) and H_L (0.80) obtained in this study to their data and estimated their cardiac output curve, the estimated cardiac output closely correlates with the values measured (y = 0.67 x + 29.0, r^2 = 0.90, SEE = 5.0 ml·min^{-1}·kg^{-1}, from 40 to 150 ml·min^{-1}·kg^{-1}).

Clinical application of the framework of circulatory equilibrium

Cardiac patients frequently receive empirical fluid challenges to treat low cardiac output, unexplained hypotension, and oliguria (1, 32). Such empirical challenges sometimes exert deleterious effect by excessive volume expansion (1, 32). Our framework is free of such problems. That is because we can accurately estimate the stressed blood volume of the patient and predict hemodynamics resulting from the volume challenge once we measure a single set of steady-state CO, P_{LA} and P_{RA} values with for example, Swan-Ganz catheters (2).

The outcome of acute or chronic heart failure has been related to the severity of reduced cardiac output and elevated left ventricular filling pressure (4, 5, 13, 23). Several studies, however, indicate that having Forrester class IV hemodynamics does not necessarily condemn patients to a class IV prognosis. Even if the initial hemodynamics are classified as class IV, patients showing reduction in filling pressure following intensive medical therapy have a better prognosis than those without reduction in filling pressure (13, 23). Using our framework for guidance, proper management of low cardiac output and elevated filling pressures would improve the prognosis of such patients.

In clinical settings, the reference point for zero pressure is determined by an empirical external inspection (16). Changes in the patient's position relative to the pressure transducer may induce apparent changes in atrial pressures (16). These factors can result in a measurement error for atrial pressure, and consequently, an error in the prediction of the circulatory equilibrium. Accurate determination of the external reference point relative to the level of the right atrium and paying strict attention to patient position are required for clinical application of our framework.

Limitations of this study

All the experiments of this study were conducted in anesthetized, open-chest dogs.

Anesthesia and surgical trauma significantly affect the cardiovascular system (31). Whether this equilibrium framework can be applied to conscious, closed-chest animals (including humans) remains to be tested.

We isolated baroreceptors and fixed the autonomic tone in this study. This was necessary because the baroreflex alters the cardiac output curve and venous return surface, through its effects on stressed blood volume, vascular resistance, heart rate and cardiac contractility (8, 22). How changes in autonomic tone under the closed loop condition affect the accuracy of hemodynamic prediction remains to be investigated.

Conclusion

The integrated cardiac output curve can be estimated based on a single set of hemodynamic measurements (CO, P_{LA} and P_{RA}). The integrated cardiac output curve thus estimated enables accurate prediction of hemodynamics (CO, P_{LA} and P_{RA}) following extensive changes in stressed blood volume under heart failure conditions as well as during normal cardiac functions.

APPENDIX

Mathematical modeling of the Cardiac Output Curve

We derived the relationship between cardiac output (*CO*) and atrial pressure based on the ventricular pressure-volume relationship framework (15, 25) and the ventricular-arterial coupling framework (26) as follows.

The relationship between the stroke volume (*SV*) and the ventricular end-diastolic volume (V_{ed}) has been approximated with reasonable accuracy as

$$SV = \frac{TE_{es}}{TE_{es} + R} \times (V_{ed} - V_0) \tag{A1}$$

where E_{es} is the slope (elastance) and V_0 is the volume axis intercept of the ventricular end-systolic pressure-volume relationship, T is the heart period and R is the arterial resistance (20, 25, 26). Dividing SV by T, cardiac output (*CO*) can be expressed as

$$CO = \frac{E_{es}}{TE_{es} + R} \times (V_{ed} - V_0) \tag{A2}$$

V_{ed} can be interrelated with end-diastolic pressure (P_{ed}) by:

$$P_{ed} = \alpha e^{kV_{ed}} + \beta \tag{A3}$$

where k, α, and β are constants (6, 7). If we approximate P_{ed} by a scaled mean atrial pressure (P_{At}), γP_{At} (γ is a proportionality constant), *Equation A2* can be rewritten as

$$CO = \frac{1}{k} \cdot \frac{E_{es}}{TE_{es} + R} \times \left[\ln\left(P_{At} - \frac{\beta}{\gamma} \right) + \ln\left(\frac{\gamma}{\alpha} \right) - kV_0 \right] \tag{A4}$$

Equation A4 can be simplified by lumping parameters for cardiovascular system properties into

three constants, S, F, and H.

$$CO = S \times \left[\ln\left(P_{At} - F\right) + H\right] \tag{A5}$$

GRANTS

This study was supported by Health and Labor Sciences Research Grants for research on medical devices for analyzing, supporting and substituting the function of the human body and research on advanced medical technology from the Ministry of Health Labour and Welfare of Japan, a Grant-in-Aid for Scientific Research (A 15200040, C 14570707, C 15590786) from the Japan Society for the Promotion of Science, and a Grant-in-Aid for Young Scientists (B)(16700379) from the Ministry of Education, Culture, Sports, Science and Technology, as well as by the Program for Promotion of Fundamental Studies in Health Science of Pharmaceuticals and Medical Devices Agency of Japan.

REFERENCES

1. **Bendjelid K, Suter PM, and Romand JA.** The respiratory change in preejection period: a new method to predict fluid responsiveness. *J Appl Physiol* 96: 337-342, 2004.
2. **Chaliki HP, Hurrell DG, Nishimura RA, Reinke RA, and Appleton CP.** Pulmonary venous pressure: relationship to pulmonary artery, pulmonary wedge, and left atrial pressure in normal, lightly sedated dogs. *Catheter Cardiovasc Interv* 56: 432-438, 2002.
3. **Chen CH, Fetics B, Nevo E, Rochitte CE, Chiou KR, Ding PA, Kawaguchi M, and Kass DA.** Noninvasive single-beat determination of left ventricular end-systolic elastance in humans. *J Am Coll Cardiol* 38: 2028-2034, 2001.
4. **Crexells C, Chatterjee K, Forrester JS, Dikshit K, and Swan HJ.** Optimal level of filling pressure in the left side of the heart in acute myocardial infarction. *N Engl J Med* 289: 1263-1266, 1973.
5. **Forrester JS, Diamond G, Chatterjee K, and Swan HJG.** Medical therapy of acute myocardial infarction by application of hemodynamic subsets (first of two parts). *N Eng J Med* 295: 1356-1362, 1976.
6. **Glantz SA, and Kernoff RS.** Muscle stiffness determined from canine left ventricular pressure-volume curves. *Circ Res* 37: 787-794, 1975.
7. **Glantz SA, and Parmley WW.** Factors which affect the diastolic pressure-volume curve. *Circ Res* 42: 171-180, 1978.
8. **Greene AS, and Shoukas AA.** Changes in canine cardiac function and venous return curves by the carotid baroreflex. *Am J Physiol* 251: H288-H296, 1986.
9. **Guyton AC.** Determination of cardiac output by equating venous return curves with cardiac response curves. *Physiol Rev* 35:123-129, 1955.